Published in final edited form as:
Hippocampus. 2011 December ; 21(12): 1302–1317. doi:10.1002/hipo.20842.

High affinity group III mGluRs regulate mossy fiber input to CA3 interneurons

Kathleen E. Cosgrove, **Stephen D. Meriney**, and **Germán Barrionuevo**
Department of Neuroscience, University of Pittsburgh, Pittsburgh, Pennsylvania 15260, and Center for Neuroscience, University of Pittsburgh, Pittsburgh, PA 15260

Abstract

Stratum lacunosum-moleculare interneurons (L-Mi) in hippocampal area CA3 target the apical dendrite of pyramidal cells providing feedforward inhibition. Here we report that selective activation of group III metabotropic glutamate receptors (mGluRs) 4/8 with L-(+)-2-amino-4-phosphnobytyric acid (L-AP4; 10 μM) decreased the probability of glutamate release from the mossy fiber (MF) terminals synapsing onto L-Mi. Consistent with this interpretation, application of L-AP4 in the presence of 3 mM strontium decreased the frequency of asynchronous MF EPSCs in L-Mi. Furthermore, the dose response curve showed that L-AP4 at 400 μM produced no further decrease in MF EPSC amplitude compared to 20 μM L-AP4, indicating the lack of mGluRs 7 at these MF terminals. We also found that one mechanism of mGluRs 4/8-mediated inhibition of release is linked to N-type voltage gated calcium channels at MF terminals. Application of the group III mGluR antagonist MSOP (100 μM) demonstrated that mGluRs 4/8 are neither tonically active nor activated by low and moderate frequencies of activity. However, trains of stimuli to the MF at 20 and 40Hz delivered during the application of MSOP revealed a relief of inhibition of transmitter release and an increase in the overall probability of action potential firing in the postsynaptic L-Mi. Interestingly, the time to first action potential was significantly shorter in the presence of MSOP, indicating that mGluR 4/8 activation delays L-Mi firing in response to MF activity. Taken together, our data demonstrate that the timing and probability of action potentials in L-Mi evoked by MF synaptic input is regulated by the activation of presynaptic high affinity group III mGluRs.

Keywords

feedforward; short term plasticity; frequency facilitation; str. lacunosum-moleculare

Introduction

The main sources of extrinsic excitatory input to area CA3 of the hippocampus are the perforant path (PP) from the entorhinal cortex, and the mossy fibers (MF) from the dentate gyrus. In addition, the CA3 network receives a strong intrinsic excitatory input from the associational connections via the recurrent axon collaterals (RC) of CA3 pyramidal cells. Under normal conditions, the excitatory drive from these three inputs is regulated by feedforward and feedback inhibition mediated by local GABAergic interneurons. Under pathological conditions like epilepsy, the balance between excitation and inhibition is disrupted (Avoli et al., 2002). Recent epilepsy research indicates that metabotropic

Correspondence should be addressed to: Germán Barrionuevo, Department of Neuroscience, A210 Langley Hall, University of Pittsburgh, PA. 15260; Phone: (412) 624-7330; Fax: (412) 624-9198. german@pitt.edu.

glutamate receptors (mGluRs) may be a therapeutic target because they modulate both excitatory and inhibitory circuits in the hippocampus (Schoepp, 2001; Tang, 2005).

Metabotropic glutamate receptors fall into three distinct groups based on amino acid sequence and sensitivity to specific agonists (Conn and Pin, 1997). Group I mGluRs increase phospholipase C activity, and groups II and III inhibit adenylyl cyclase activity (Cartmell and Schoepp, 2000; Conn and Pin, 1997). Group III mGluRs are sensitive to the agonist L-(+)-2-amino-4-phosphnobytyric acid (L-AP4) at varying concentrations (Conn and Pin, 1997). Both L-AP4 and glutamate activate mGluRs 4 and 8 at much lower concentrations than those required to activate mGluR 7 (Conn and Pin, 1997). Anatomical data indicate that within the hippocampus, group III mGluRs are commonly found presynaptically within the active zone of asymmetric synapses (Bradley et al., 1999; Shigemoto et al., 1997). When expressed presynaptically, mGluRs reduce synaptic transmission through a variety of mechanisms including modulation of ion channels, and phosphorylation of proteins in the release machinery (Anwyl, 1999; Cartmell and Schoepp, 2000). Additionally, mGluRs are frequently expressed differentially on axon terminals based on the identity of the target cell (Rusakov et al., 2004; Scanziani et al., 1998; Semyanov and Kullmann, 2000; Toth and McBain, 2000).

Previous investigations into the functional role of group III mGluRs in CA3 of the hippocampus have focused on mGluR 7 (Corti et al., 2002; Pelkey et al., 2005; Shigemoto et al., 1997). MF boutons containing mGluR 7 target interneurons within the str. lucidum, but not pyramidal cells (Pelkey et al., 2005; Shigemoto et al., 1997). Because not all MF terminals targeting interneurons express mGluR 7 (Shigemoto et al., 1997) we hypothesized that presynaptic expression of group III mGluRs on MF boutons contacting interneurons is target-cell specific.

Here we investigated whether MF input to feedforward inhibitory interneurons with soma in the str. lacunosum moleculare (L-Mi) is modulated by group III mGluRs. Previously we have shown that L-Mi receive MF input on dendrites near the suprapyramidal blade of the dentate gyrus, and on ventral dendrites extending into the str. lucidum (Cosgrove et al., 2009). We now report that L-Mi are targeted by MF terminals which do not express mGluR 7 but are modulated by mGluRs 4/8. Although the ability of mGluRs 4/8 to modulate presynaptic release characteristics has been investigated at other synapses in the hippocampus, few have addressed the impact of that modulation on the network. Here, we complemented the application of L-AP4 with the use of the antagonist, MSOP, to determine the role of the receptor in response to endogenous glutamate release during patterns of MF activity that fall within a physiologic range (Henze et al., 2002; Jung and McNaughton, 1993). Using the antagonist, we report that activation of mGluRs 4/8 by high frequency MF activity delays spike transmission between the MF and L-Mi, thus delaying the onset of feedforward inhibition in CA3 pyramidal cells. These results highlight the physiologic importance of presynaptic mGluRs in regulating feedforward inhibition in area CA3 of the hippocampus.

Materials and Methods

Hippocampal slice preparation

Slices were prepared as described previously (Calixto et al., 2008). Briefly, Male Sprague-Dawley rats (21–28 days old; Charles River) were deeply anaesthetized (Nembutal, I.P., 5mg per 100 g body weight) and perfused intracardially with cold (4°C) modified artificial cerebrospinal fluid (ACSF) in which sodium chloride was replaced with sucrose (concentration in mM: 210 sucrose, 2.8 KCl, 2 $MgSO_4$, 1.25 Na_2PO_4, 26 $NaHCOO_3$, 10 glucose, 1 $CaCl_2$, 1 $MgCl_2$, pH 7.3, continuously bubbled with 95% O_2 / 5% CO_2).

Following 30 sec to 1 min of perfusion, animals were decapitated and the brain removed. The brains were sliced using a Leica VT1000S vibratome and were cut in 320–340 μm sections. Slices were transferred to an incubation solution (in mM: 125 NaCl, 2.5 KCl, 1.25 Na_2PO_4, 25 $NaHCOO_3$, 10 glucose, 1 $CaCl_2$, 4 $MgCl_2$, 0.4 L-ascorbic acid, pH 7.3), continuously bubbled with 95% O_2 / 5% CO_2 at 32°C for 30 min, and then allowed to return to room temperature for at least 30 min before beginning recording. The slices were then transferred to a submersion recording chamber and superfused at a constant flow (2.5 mL / min) with ACSF (in mM: 125 NaCl, 2.5 KCl, 1.25 Na_2PO_4, 25 $NaHCO_3$, 10 glucose, 2 $CaCl_2$, 2 $MgCl_2$, pH 7.3) via a peristaltic pump (Watson Marlow 400 series). All recording were made at 32 – 34°C and in the presence of 10 μM bicuculine and 50 μM D-2-amino-5-phosphonopentanoic acid (D,L–AP5) unless otherwise noted. All animal use was in accordance with the University Institutional Animal Care and Use Committee at the Univ. of Pittsburgh.

Electrophysiological recording methods

Whole cell recordings were made from the soma of putative interneurons in the str. lacunosum moleculare of CA3b of the hippocampus. Cell bodies were localized 50 – 100 μm from the slice surface and identified visually using infrared video microscopy and differential interference contrast optics. Patch pipettes with resistances of 2 – 5 M were pulled from borosilicate glass and filled with a solution containing (in mM): 120 $KMeSO_4$, 10 KCl, 10 HEPES, 0.5 EGTA, 4 MgATP, 0.3 Na_2GTP, 8 phosphocreatine. Biocytin (0.2%) was routinely added to the pipette solution to allow subsequent morphological identification and reconstruction of the neurons. All recordings were obtained using an Axopatch 200B amplifier (Axon Instruments, Foster City, CA, USA). Signals were low pass filtered at 2 kHz, digitized at 10 kHz and stored on disk for off-line analysis. Data acquisition and analysis were performed using the pClamp 10 suite of software (Molecular Devices). Series resistance was monitored throughout recordings and experiments were discontinued if resistance increased by > 15%. Whole cell voltage-clamp recordings were held at −60 mV and in current clamp the cell was maintained within ~ 3 mV of rest unless otherwise noted. Cell attached recordings were made using pipettes with a resistance of 3 – 5 MΩ with ACSF as the internal solution. These recordings were made in voltage clamp as described by Perkins (2006) in loose patch mode (seal resistance: 100 – 500 MΩ).

The MF pathway was stimulated extracellularly using a concentric bipolar electrode (FH-US) positioned either at the medial extent of the suprapyramidal blade of the dentate gyrus (MF_{SDG}) or within the s. lucidum dorsal to the ventral tip of the dentate gyrus (MF_{SL}; Fig. 1A). In every experiment, the group II metabotropic glutamate receptor agonist (2S,2’R,3’R) – 2 – (2’,3’ – dicarboxycyclopropyl) glycine (DCG-IV; 1 – 2.5 μM) was applied and responses were classified as of MF origin if DCG-IV decreased the postsynaptic response by > 50% (Alle et al., 2001;Galvan et al., 2008;Lawrence et al., 2004). The recurrent collaterals were stimulated by an electrode positioned within the str. oriens of CA3. Synaptic responses were evoked by low intensity stimulation (10 to 300 μA intensity, 100 μs duration) via a constant-current isolation unit (Wesco, SC-100). Responses were included in analysis only if the rate of rise could be fit with a single exponential that lacked any obvious multiple EPSC or polysynaptic waveforms. Paired pulse ratio was determined using the calculation $EPSC_2$ / $EPSC_1$.

Selection criteria and analysis of asynchronous EPSCs

Experiments using strontium to determine the quantal amplitude of the MF response were performed with a modified internal solution that replaced K^+ with Cs^+ (in mM): 120 $CsMeSO_4$, 10 KCl, 10 HEPES, 0.5 EGTA, 4 MgATP, 0.3 Na_2GTP, 8 phosphocreatine. Bath solution was altered to contain 0 Ca^{2+} and 8mM Sr^{2+} (Bekkers and Clements, 1999; Goda

and Stevens, 1994; Lawrence et al., 2004). The MF was stimulated and asynchronous EPSCs (aEPSCs) were selected as follows. The time from the stimulus to the beginning of each event was calculated and plotted in a histogram, excluding the synchronous event (Supplemental Fig. 1). The histogram was then fit with a single exponential decay, and the value of the offset was considered to be the background frequency (indicated by the arrow in Supplemental Fig. 1B). The 95% confidence interval of the offset was calculated and extrapolated horizontally back to the y-axis (Supplemental Fig. 1B, red line). The time at which the fitted decay crossed the 95% confidence interval of the offset was considered to be the cutoff time (Supplemental Fig. 1B, t_c: 517.28 ± 100.32 ms, N = 10). Only events that occurred prior to t_c were considered to be aEPSCs evoked by MF stimulation and included in the analysis. To determine the mean quantal amplitude, the peak amplitudes of each aEPSC were plotted in a histogram (Supplemental Fig. 1C). This histogram was then fit with a single Gaussian function to determine the quantal amplitude (mean) for each input (Bekkers and Clements, 1999).

Statistics

Statistical significance was set at $p < 0.05$ and determined through the use of Student's t-test or ANOVA (when multiple comparisons were made). Amplitude distributions of aEPSCs were tested using Kolmolgorov-Smirnov test.

Drugs

Bicuculine, AP5, L-AP4, DCG-IV, MSOP, OH-Saclofen were obtained from Tocris (Ellisville, MO). All other compounds were obtained from Sigma Aldrich (St. Louis, MO).

Results

Interneurons with soma residing in the str. lacunosum moleculare have wide spread dendritic and axonal arbors. Dendrites extend horizontally through the str. lacunosum moleculare and ventrally into the str. lucidum (Ascoli et al., 2009) receiving MF input on both the dorsal and ventral dendritic arbors (Cosgrove et al., 2009). Axonal arbors of L-Mi are complex and extend throughout the str. radiatum (Ascoli et al., 2009), presumably contacting CA3 pyramidal cells along the apical dendrite, providing feedforward inhibition (Lacaille and Schwartzkroin, 1988; Williams et al., 1994). To determine whether MF input to L-Mi is regulated by group III mGluRs, recordings were made from visually identified L-Mi and the mossy fiber was stimulated both within the str. lucidum (MF_{SL}), and at the suprapyramidal blade of the dentate gyrus (MF_{SDG}; Fig. 1A; Cosgrove et al., 2009; Galvan et al., 2008; Galvan et al., 2010). The origin of EPSCs was confirmed to be MF by application of the group II mGluRs agonist DCG-IV (Kamiya et al., 1996). While DGC-IV inhibition of MF transmission in pyramidal cells is consistently complete (≥90%; Kamiya et al., 1996), it is partial in interneurons. For example, Alle et al. (2001) observed a reduction of about 70% for both the composite and unitary postsynaptic responses obtained from paired recordings. Thus, EPSCs in L-Mi were considered of MF origin if the percent decrease from DCG-IV application was greater than 50%, a measure that has been used previously (Cosgrove et al., 2009; Galvan et al., 2008; Galvan et al., 2010; Lawrence et al., 2004; Toth et al., 2000).

High affinity group III mGluRs are present on MF terminals contacting L-Mi

Receptors belonging to group III mGluRs are mGluRs 4, 6, 7 and 8 and are activated by the agonist L-AP4 (Conn and Pin, 1997). Of those receptors, mGluRs 4, 7 and 8 are expressed in the hippocampus (Saugstad et al., 1994; Shigemoto et al., 1997; Tanabe et al., 1993). Previous reports indicate that MF input to str. lucidum interneurons is modulated by mGluR 7, the low affinity group III mGluRs (Pelkey et al., 2005) which binds glutamate in the 1 mM range and L-AP4 at 160 to 500 μM (Conn and Pin, 1997). To determine whether this

receptor is also present on MF terminals contacting L-Mi, we performed a dose-response curve using the group III mGluR agonist L-AP4 (Fig. 1B). Surprisingly, we found no evidence for the presence of mGluR 7, but did find evidence for the presence of high affinity group III mGluRs 4 and 8, which have an affinity for glutamate near 3–38 μM, and for L-AP4 in the 1 – 2 μM range (Conn and Pin, 1997). Specifically, the dose response curve shows that L-AP4 at 400 μM produced no further decrease in EPSC amplitude compared to L-AP4 at 20 μM, a saturating dose for mGluRs 4/ 8 that is insufficient to activate mGluR 7 (400 μM: 31.93 ± 7.13% of control, N = 5; 20 μM: 32.30 ± 6.47% of control, N = 9; p = 0.971; Fig. 1B). Though these data do not conclusively exclude the presence of mGluR 7, they do reveal the novel presence of high affinity group III mGluRs 4/8 at a MF to interneuron synapse.

In the next series of experiments, we applied 10 μM L-AP4 to ensure that we were selectively activating mGluRs 4/8, and also stimulated the RC pathway of CA3, which has been shown to be relatively insensitive to mGluRs agonists (Kamiya et al., 1996; Toth and McBain, 1998; but see Doherty and Dingledine, 1998). EPSCs evoked by MF stimulation decreased by 45.65 ± 5.47% (N = 12, $p < 0.001$) in the presence of 10 μM L-AP4 and was fully reversible (93.38 ± 4.34% of control, p = 0.183; Fig. 1C and 1F, blue bars). For this sample of cells, the group II mGluR agonist DCG-IV (1 μM) decreased EPSCs by 67.75 ± 4.34% (N = 12, $p < 0.001$), which is similar to the effect of DCG-IV on MF-evoked responses in other interneurons (Alle et al., 2001; Lawrence et al., 2004; Toth et al., 2000). In contrast, EPSCs evoked by RC stimulation did not change in response to either L-AP4 or DCG-IV application (L-AP4: 2.71 ± 5.92% decrease, p = 0.666; DCG-IV: 4.45 ± 5.14% decrease, p = 0.426; N = 6; Fig. 1D and 1F, red bars). Though RC and MF axons cross in the str. lucidum of CA3, it is unlikely that RC inputs were activated by the MF_{SL} stimulation location since both the MF_{SL} and MF_{SDG} stimulation locations had the same DCG-IV sensitivity (Table 1). Interestingly, the decrease in EPSC amplitude with 10 μM L-AP4 was similar to that previously reported at the MF to pyramidal cell synapse of the guinea pig (Manzoni et al., 1995; Yoshino et al., 1996) and at the granule cell input to hilar border interneurons (Doherty and Dingledine, 1998).

In a subset of these cells, the control recordings had a failure rate of at least 10%. For these cells, we analyzed the failure rate, paired-pulse ratio and coefficient of variation before and after the application of 10 μM L-AP4. As would be expected from a presynaptically mediated depression, application of L-AP4 increased the failure rate (21.0 ± 6.23% control to 66.45 ± 11.47% L-AP4; $p < 0.01$; N = 6), paired-pulse ratio (1.04 ± .05 control to 1.54 ± .14 L-AP4; $p < 0.01$; N = 5) and coefficient of variation (0.535 ± 0.08 control to 0.857 ± 0.208; $p < 0.05$; N = 6) indicating that activation of mGluRs 4/8 decreased the probability of transmitter release (Fig. 1E).

Since MFs are pharmacologically identified through the application of the group II mGluRs agonist DCG-IV (Kamiya et al., 1996), and both group II and group III mGluRs have been shown to inhibit adenylyl cyclase (Cartmell and Schoepp, 2000; Conn and Pin, 1997), we wanted to know whether activation of mGluRs 4/8 on MF terminals by L-AP4 occluded the actions of DCG-IV on group II mGluRs. In a separate group of cells, we first applied L-AP4 and then DCG-IV without a washout period. In these experiments, L-AP4 did not occlude the actions of DCG-IV. Following application of 10 μM L-AP4 (38.28 ± 4.2% decrease, N = 10), DCG-IV caused a further decrease of 66.08 ± 5.32% in EPSC amplitude ($p < 0.001$; N = 10; Fig. 2). Additionally, since 10 μM L-AP4 was not a maximal concentration (see Fig. 1), the effect of DCG-IV after L-AP4 application was compared to the effect of DCG-IV alone (previous experiment). There was no significant difference in the inhibition produced by DCG-IV alone (67.75 ± 4.34%; N = 12) vs. DCG-IV after L-AP4 (66.08 ± 5.32%; N = 10; p = 0.967; Fig 2C).

Both the increase in failure rate and PPR as a result of L-AP4 application suggests a presynaptic localization of mGluRs 4/8 at the MF – L-Mi synapse, an interpretation supported by anatomical studies (Bradley et al., 1999; Shigemoto et al., 1997; but see Bradley et al., 1996). To obtain direct confirmation of the presynaptic localization of the receptor, we bath applied Sr^{2+} (see Methods) to de-synchronize the evoked release into putative single quanta (Bekkers and Clements, 1999; Goda and Stevens, 1994; Lawrence et al., 2004). The amplitude distribution of asynchronous EPSCs (aESPCs; see Methods) revealed a quantal amplitude of 7.88 ± 0.29 pA (range: 6.70 pA to 9.59 pA; N = 10; Supplemental Fig. 1D; Table 1), a value similarly found at other central synapses (Bekkers and Clements, 1999; Jonas et al., 1993) but significantly smaller than the quantal amplitude for the MF synapse on str. lucidum interneurons (mean: 24.5 pA; Lawrence et al., 2004). To confirm that activation of mGluRs 4/8 had a presynaptic effect, we assessed the effect of L-AP4 (10 μM) on the amplitude and frequency of aEPSCs (Price et al., 2005) in a separate group of cells. In the presence of 3 mM Sr^{2+}, L-AP4 application decreased the frequency of aEPSCs following stimulation (3.72 ± 0.72 Hz in control vs. 2.30 ± 0.30 Hz after L-AP4; $p < 0.05$; N = 7) without changing the amplitude (7.09 ± 0.40 pA control vs. 7.73 ± 0.61 pA L-AP4; $p = 0.389$; N = 7; Fig. 3). In addition to comparing the mean amplitudes, the distribution of aEPSC amplitudes within each cell was compared before and after application of L-AP4 to ensure that no change in the distributions of aEPSC amplitudes was observed (Fig 3B; $p = 0.198$). None of the cells tested showed any significant difference in the distribution of aEPSC amplitudes ($p \geq 0.198$ for all cells), confirming the lack of effect of L-AP4 on aEPSC amplitude. The effect on frequency was fully reversible (3.84 ± 0.33 Hz after washout). The lack of change in aEPSC amplitude combined with a significant decrease in frequency indicates that activation of mGluRs 4/8 decreases the probability of release without affecting the postsynaptic cell (Price et al., 2005).

Because PP synaptic responses are sensitive to both group II and group III mGluRs, it could be argued that electrical stimulation applied to MF_{SDG} could also evoke PP EPSCs. This is unlikely for the following reasons. First, the medial and lateral PPs are modulated by different mGluRs, the medial PP by group II mGluRs and the lateral PP by group III mGluRs, but not both (Macek et al., 1996). The postsynaptic responses that were evoked from MF_{SDG} stimulation were highly sensitive to agonists of both group II and group III mGluRs. Additionally, when the MF was stimulated within the str. lucidum (MF_{SL}) activating synapses far from the str. lacunosum-moleculare (Cosgrove et al., 2009), the sensitivity to L-AP4 was identical to stimulation at the MF_{SDG} (Table 1). Together, these data support the claim that glutamate release from MF onto L-Mi is modulated by mGluRs 4/8. This novel finding indicates the presence of high affinity group III mGluRs at MF terminals targeting a specific feedforward inhibitory interneuron, suggesting that L-Mi serve unique functional roles in the CA3 neural network.

The N-type calcium channel is a target of high affinity group III mGluRs at the MF to L-Mi synapse

Presynaptic receptors commonly regulate transmitter release by modulating the voltage-gated calcium channels (VGCCs) linked to release (Ferraguti and Shigemoto, 2006; Takahashi et al., 1996). Group III mGluRs inhibit adenylyl cyclase, decreasing the activity of protein kinase A (PKA) which has been shown to target VGCCs (Anwyl, 1999; de Jong and Verhage, 2009). In contrast, group II mGluRs are frequently found to inhibit transmitter release through VGCC-independent mechanisms (Anwyl, 1999; Capogna, 2004; Glitsch, 2006; Knöpfel and Uusisaari, 2008). Since application of L-AP4 did not occlude the action of DCG-IV at the MF to L-Mi synapse, we hypothesized that mGluRs 4/8 activation results in inhibition of VGCCs, whereas activation of group II mGluRs would not, further confirming the independence of their intracellular signaling cascades. To determine whether

VGCCs are a downstream target of mGluRs 4/8 or mGluRs 2/3 activation at the MF to L-Mi synapse, we first determined the complement of VGCCs linked to release of glutamate at MF to L-Mi synapses. Using specific toxins to isolate the P/Q- and N-type calcium channels, we found that glutamate release at the MF to L-Mi connection is largely dependent on P/Q-type VGCCs, as previously reported for the MF to pyramidal cell, and MF to str. lucidum interneuron connections (Breustedt et al., 2003; Castillo et al., 1994; Li et al., 2007; Miyazaki et al., 2005; Pelkey et al., 2006). Specifically, we found that glutamate release was predominantly linked to P/Q-type channels (ω-agatoxin IVA decreased EPSC amplitude by 83.1 ± 2.4%; N = 13; $p < 0.0001$) with a smaller but significant contribution from N-type VGCCs (ω-conotoxin GVIA decreased EPSC amplitude by 27.29 ± 5.5%, N = 18; $p < 0.001$; Fig. 4A).

Next, we assessed whether N-type or P/Q-type VGCCs were downstream targets of mGluRs 4/8 or mGluRs 2/3 activation by applying L-AP4 or DCG-IV, respectively, after selectively blocking the N- or P/Q-type VGCCs. DCG-IV decreased EPSC amplitude by 63.75 ± 7.14% (N = 7) in the presence of ω-CgTx and 63.35 ± 5.94% (N = 6) in the presence of ω-AgaTx, indicating that neither VGCC blocker occluded the effect of DCG-IV (Fig. 4B). Furthermore, in comparing the effect of DCG-IV in the presence of the selective VGCC blockers to the effect of DCG-IV alone (decrease of 67.75 ± 4.34%, N = 11, value from previous experiment, see Fig. 1), there was no significant difference in the percent decrease ($p = 0.812$, Fig. 4C), indicating that activation of mGluRs 2/3 does not involve N- or P/Q-type VGCCs as a downstream target.

In contrast to what was seen with DCG-IV, application of L-AP4 in the continued presence of the selective VGCC blockers did indicate that the N-type VGCC is a downstream target of mGluRs 4/8 activation. L-AP4 decreased EPSC amplitude by 28.05 ± 4.90% (N = 10) in the presence of ω-CgTx, but caused a decrease of 62.0 ± 11.69% (N = 7; $p < 0.01$; Fig. 4D) in the presence of ω-AgaTx. These data indicate that activation of mGluRs 4/8 results in selective inhibition of glutamate release linked to N-type VGCCs, which is a similar to what has been reported at other synapses (Rusakov et al., 2004). Additionally, when these data are compared to the effect of 10 μM L-AP4 in the absence of a VGCC blocker, the effect of L-AP4 after blockade of N-type VGCCs is significantly smaller, indicating that ω-CgTx partially occludes the effects of L-AP4 (L-AP4 after CgTx: 28.05 ± 4.90% decrease; N = 10 vs. L-AP4 alone: 45.65 ± 5.47% decrease; N = 11; $p < 0.05$; value from previous experiment, see Fig. 1; Fig. 4E).

Since there was large variability in the effect of ω-CgTx at MF to L-Mi synapses, determining whether the effect of L-AP4 was occluded by blocking N-type VGCCs was difficult because in some cells N-type VGCCs were not linked to release, as the effect of ω-CgTx was very small (Fig. 4F). If mGluRs 4/8 selectively target glutamate release linked to N-type over P/Q-type VGCCs, we hypothesized that there would be a correlation between the effects of ω-CgTx and L-AP4 in the continued presence of ω-CgTx. To investigate this, the percent decrease in EPSC amplitude following L-AP4 application in the continued presence of ω-CgTx was plotted vs. the percent decrease in EPSC amplitude produced by the application of ω-CgTx alone. As shown in Figure 4F, we obtained a significant correlation (slope: −42.75 ± 4.44; N = 10; R = −0.832; $p < 0.01$) such that when ω-CgTx had its largest effect (% decrease near 50%), L-AP4 application resulted in no further decrease in EPSC amplitude (% decrease near 10%; Fig 4F, square symbol and traces).

Interestingly, however, these data also indicate a second, N-type VGCC-independent mechanism through which mGluRs 4/8 inhibit transmitter release at the MF to L-Mi synapse. In a subset of cells that were relatively ω-CgTx resistant (% decrease ≤ 20%, Fig 4F, triangle symbol and trace) indicating that N-type VGCCs were not linked to glutamate

release, the effect of L-AP4 was similar to the effect of L-AP4 in the absence of VGCCs blockers (effect of L-AP4 in ω-CgTx resistant cells: −39.08 ± 4.11%, N=4 vs. effect of L-AP4 alone from previous experiment: −45.65 ± 5.47%, N =11; p = 0.504). Thus, it can be concluded that in terminals where N-type VGCCs are linked to transmitter release at the MF to L-Mi connection, the N-type VGCC is a downstream target of mGluRs 4/8 activation (e.g. Fig. 4F, square symbol and traces). If N-type VGCCs are not linked to glutamate release however, mGluRs 4/8 activation is equally effective at decreasing glutamate release (e.g. 4F, triangle symbol and traces), possibly through a direct action on the release machinery, as proposed by others (Anwyl, 1999;Scanziani et al., 1995;Schoppa and Westbrook, 1997;Woodhall et al., 2007).

Low frequency activity is insufficient to activate high affinity group III mGluRs

Application of the agonist L-AP4 to synapses with high affinity group III mGluRs frequently overestimates the endogenous impact of this receptor on the system (Billups et al., 2005; Lorez et al., 2003; von Gersdorff et al., 1997). Thus, to determine the functional impact of this receptor at the MF to L-Mi connection, we used the competitive antagonist of group III mGluRs, MSOP (100 μM), to prevent endogenous activation (Rusakov et al., 2004; Semyanov and Kullmann, 2000; Thomas et al., 1996). To assess the pattern of activity that might physiologically activate the receptor, we investigated whether the receptor was tonically active and whether it could be activated by low or high frequency activity.

To assess tonic activity, MSOP (100 μM) was applied and the effect on the amplitude of single postsynaptic responses was determined. No effect on the initial amplitude of the postsynaptic response was seen using a test frequency of 0.2 Hz (23.94 ± 2.69 pA control; 23.83 ± 3.14 pA MSOP; p = 0.950; N = 9; Fig. 5C). This was also true for responses recorded in current clamp (amplitude: 1.59 ± 0.57 mV control; 1.48 ± 0.68 mV MSOP; N = 5; p = 0.279; Fig. 5C). These data indicate that the group III mGluRs are not tonically active on MF terminals contacting L-Mi, suggesting that ambient extracellular glutamate concentrations are insufficient to activate the receptor.

Since mGluRs 4/8 have a high affinity for glutamate, these receptors could be activated by low frequency MF discharge. At other targets, the MF input exhibits frequency facilitation, an increase in the amplitude of the postsynaptic response as the stimulation frequency increases from very low (0.05 Hz) to more moderate (1 – 4 Hz; Henze et al., 2000; Salin et al., 1996). MF input to pyramidal cells undergoes robust facilitation at low and moderate frequencies that can exceed 600% at 4 Hz vs. 0.05 Hz (Henze et al., 2000; Salin et al., 1996; Scanziani et al., 1998; Toth et al., 2000). Similarly, it has been reported that mossy fiber input to str. lucidum interneurons exhibits strong frequency facilitation (Toth et al., 2000). To investigate whether glutamate release by low to moderate frequencies of MF activity were sufficient to activate mGluRs 4/8 at the MF to L-Mi synapse, we recorded MF-evoked EPSCs in L-Mi at stimulation frequencies from 0.05 to 4Hz (Salin et al., 1996). In contrast to MF responses in pyramidal cells and str. lucidum interneurons, we did not detect a significant increase in EPSC amplitudes at 4 Hz compared to the 0.05 Hz control (1.09 ± 0.12 normalized to 0.05 Hz control; p = 0.460; N = 8; Fig. 5A, B).

Although we did not observe frequency facilitation in the control condition, it is possible that application of MSOP (100 μM) might reveal an underlying facilitation at moderate frequencies (Scanziani et al., 1997; Toth et al., 2000). To test this hypothesis, we stimulated the MF with alternate periods of 0.05 Hz and 2 Hz (Scanziani et al., 1997), a frequency that shows strong facilitation at both the MF to pyramidal cell and MF to str. lucidum interneuron connections (Toth et al., 2000). Application of MSOP did not rescue frequency facilitation at the MF – L-Mi synapse tested at 2Hz (normalized to 0.05 Hz: 1.21 ± 0.10 control; 1.11 ± 0.20 MSOP; N = 5; p = 0.677; Fig. 5D). Furthermore, amplitudes at 2 Hz

were not significantly different than amplitudes at 0.05 Hz for either the control or MSOP condition (control: 28.71 ± 3.91 pA at 0.05 Hz; 34.79 ± 5.47 pA at 2 Hz; p = 0.108; N = 5; MSOP: 29.82 ± 5.46 pA at 0.05 Hz; 29.70 ± 2.83 pA at 2Hz; p = 0.972; N = 5) indicating that low and moderate frequencies are insufficient to activate this receptor.

Activation of high affinity group III mGluRs by high frequency MF activity delays the onset of L-Mi firing

Having demonstrated that mGluRs 4/8 are not tonically active at the MF to L-Mi connection, nor activated by low and moderate frequencies of activity, we were interested in determining the effect of the receptor at high frequencies of activity. Previous reports have demonstrated that short trains of high frequency activity are sufficient to activate high affinity group III mGluRs (Chen et al., 2002; Losonczy et al., 2003). To determine whether short trains of high frequency activity were sufficient to activate mGluRs 4/8 at MF input to L-Mi, we recorded trains of five MF-evoked EPSCs at 20 and 40 Hz, frequencies that fall within the range of granule cell firing as a rat traverses a place field (Henze et al., 2002; Jung and McNaughton, 1993), before and after application of MSOP.

Figure 6 shows the data from those experiments, demonstrating the facilitation ratio ($EPSC_N$ / $EPSC_1$) of the postsynaptic response for each stimulus in the train before and after application of MSOP. MSOP revealed an average enhancement of facilitation at 20 Hz, and though there was a trend at 40 Hz, the effect was not significant for most test stimuli (stimuli 2 – 5) when the data from each condition were averaged. In part, the lack of significance at all points in the 40 Hz train for these data is due to the high variability of facilitation in the control condition, as well as in the MSOP condition, as demonstrated in the averaged traces in Fig. 6. For example, in some cells the largest effect of MSOP was at stimulus #3, whereas for other cells, stimulus #5 showed the largest effect (see averaged traces in Fig. 6A and 6D). Because of the variability in the timing of the facilitation resulting from MSOP application, the averaged population data did not accurately represent the effect of MSOP on short term facilitation at the MF to L-Mi connection. Therefore, the data were aligned to the stimulus number at which the greatest difference was observed after application of MSOP. Using this method, enhanced facilitation is observed following application of 100 μM MSOP at both 20 ($EPSC_N$ / $EPSC_1$: control, 1.32 ± 0.18; MSOP, 1.79 ± 0.24; N = 8; $p < 0.001$; Fig. 6C) and 40 Hz ($EPSC_N$ / $EPSC_1$: control, 1.49 ± 0.17; MSOP, 2.05 ± 0.24; N = 7; $p < 0.05$; Fig. 6F).

Though the EPSC train data demonstrate that mGluRs 4/8 are activated by synaptically released glutamate during a physiologic pattern of high frequency MF activity, we were primarily interested in determining the effect of mGluRs 4/8 activation on the CA3 network, and specifically the ability of MF-evoked synaptic activity to elicit action potentials in the L-Mi. *In vivo* data show that short trains of high frequency MF activity can elicit action potentials in CA3 interneurons (Henze et al., 2002). Consequently, we determined the effect of MSOP on spike transmission at the MF – L-Mi connection. Based on the EPSC data in figure 6, we hypothesized that activation of mGluRs 4/8 during high frequency MF activity would modulate the MF to L-Mi connection such that activation of the receptor would result in delayed spike transmission between the MF to the L-Mi. To test this, we applied trains of ten stimuli to the MF at 20 and 40Hz before and after the application of MSOP. We then determined whether the group III receptor had an effect on the probability of action potential generation, and whether it changed the latency to the first action potential in response to the train. In these experiments, L-Mi were recorded in current clamp conditions, and the MF input was stimulated only in the MF_{SDG} location, as the MF_{SDG} stimulation location was less likely to recruit additional glutamatergic inputs throughout the train of stimuli (observation from the previous experiment). Once a stable EPSP amplitude was obtained, the V_h was adjusted between −60 mV and −55 mV to allow for a low probability of firing

(P(AP) = ~0.1) in response to 10 stimuli at 20 Hz. 30 trials of 10 stimuli at 20 and 40 Hz, delivered at 20 second intervals were then collected before and after the application of MSOP (100 μM). Fig. 7A shows several overlapping, consecutive sweeps from a representative cell, and Fig. 7B depicts the raster plot of action potentials during the train before and after MSOP application. From these data, the probability of firing in response to each stimulus in the train was calculated and the summary data plotted in Figs. 7C and 7H. We found that the overall probability of action potential firing in response to both frequencies was significantly higher in the presence of MSOP (20 Hz: 0.08 ± 0.02 control to 0.20 ± 0.05 MSOP, N = 5, $p < 0.05$; 40Hz: 0.16 ± 0.02 control to 0.21 ± 0.03 MSOP; N = 5; $p < 0.05$; Fig. 7H). At the end of the experiment, DCG-IV (2.5 μM) was applied to confirm MF origin (71.20 ± 8.37% decrease, N = 5, $p < 0.001$).

More importantly, the time to first action potential was shorter in the presence of MSOP, indicating that activation of the group III mGluRs delays the firing of the postsynaptic L-M interneuron in response to MF input. This was determined by calculating the latency to the first action potential in response to the train of MF input for each trial before and after MSOP (Fig. 8). These data were then binned by stimulus number and plotted as a cumulative scatter plot, which was fit with a Boltzmann function. MSOP application significantly decreased the time to first action potential in response to stimuli at both 20 Hz (50% control: 192.24 ± 12.0 ms; 50% MSOP: 102.02 ± 13.7 ms; $p < 0.05$; Fig. 8A) and 40 Hz (50% control: 79.71 ± 3.32 ms; 50% MSOP: 51.71 ± 1.46ms; $p < 0.05$; Fig. 8A). It is important to note that in some of the trials, the L-Mi never fired and so these numbers are an underestimate of the shift in the timing of L-Mi firing. Of equal importance is that these changes occurred without any significant change in action potential threshold (−38.26 ± 1.36 mV control; −39.28 ± 1.73 mV MSOP; N = 5; $p = 0.134$; Fig. 7I).

Because we were concerned that intracellular dialysis during whole-cell recordings may be affecting the threshold for action potential elicitation, we repeated this experiment using the cell-attached configuration in voltage clamp (seal resistance ~100 to 500 MΩ; Perkins, 2006). Nearly identical results were obtained in cell attached for both 20 Hz (probability of AP: 0.12 ± 0.01 to 0.34 ± 0.05; $p < 0.001$; N = 7; time to first AP: 150.67 ± 88.6 ms to 93.98 ± 8.93 ms; $p < 0.05$; N = 7) and 40 Hz (probability of AP: 0.25 ± 0.06 to 0.44 ± .06; $p < 0.05$; N = 7; time to first AP: 174.55 ± 5.49 ms to 47.34 ± 3.32 ms; $p < 0.05$; N = 7) confirming that this effect is due to activation of the group III mGluRs, and not heavily influenced by the recording conditions (Fig. 7 and 8).

DISCUSSION

We have demonstrated that mGluRs 4/8 mediate suppression of glutamate release at the MF synapse on L-Mi during high frequency MF discharge. This effect can be mediated through inhibition of N-type VGCCs, although it does not always require the presence of the N-type channel at MF boutons. Regardless of the mechanism, mGluRs 4/8-mediated suppression of glutamate release from the MF boutons results in delayed action potential initiation in the postsynaptic L-Mi. We also showed that MF synapses onto L-Mi have comparatively small quantal amplitudes, and are capable of undergoing paired-pulse facilitation, but not frequency facilitation. Together these results provide a novel physiological profile of the MF input to CA3 interneurons and extend our understanding of the regulation of feedforward inhibition in area CA3 of the hippocampus.

MF input to L-Mi is regulated by mGluRs 4/8

Our data demonstrating the presence of mGluRs 4/8, but not mGluR 7 at MF terminals contacting L-Mi is surprising given the documented anatomical localization of group III mGluRs in the hippocampus (Bradley et al., 1999; Corti et al., 2002; Shigemoto et al.,

1997). Anatomically, the immunolocalization of mGluR 4 on presynaptic terminals forming asymmetric synapses in CA3 is diffuse and prominent only in the inner and middle one-third of the dentate gyrus moleculare layer (Bradley et al., 1999; Corti et al., 2002; Shigemoto et al., 1997). In contrast, the distribution of mGluR 8 is pronounced in the str. lacunosum moleculare of CA3 and was attributed to the axon terminals of the lateral perforant path (Ferraguti et al., 2005; Shigemoto et al., 1997) because lesions to the entorhinal cortex decrease (though do not eliminate) this staining (Shigemoto et al., 1997). However, we have previously demonstrated spatial overlap between MF and PP synapses on L-Mi within the str. lacunosum moleculare of area CA3 (Cosgrove et al., 2009), making it possible that some of the mGluR 8 staining in the previous work may be due to granule cell axons *en route* to the str. lucidum. Supporting our contention that MF input to L-Mi is modulated by mGluRs 4/8 is the finding that mRNA for mGluRs 4 and 8 are found within the dentate gyrus granule cells (Ferraguti et al., 2005; Ohishi et al., 1995; Saugstad et al., 1997; Tanabe et al., 1993).

Furthermore, a previous electrophysiological report did not indicate the presence of mGluRs 4/8 at the MF to str. lucidum interneuron synapse but showed that this connection is specifically modulated by mGluR 7 activation (Pelkey et al., 2005; but see Doherty and Dingledine, 1998). Consistent with these data, a Ca^{2+} imaging study of the MF filopodial extensions, which are known to preferentially target interneurons (Acsady et al., 1998), demonstrated that high concentrations of L-AP4 decreased fluorescence, indicating that VGCCs are targets of mGluR 7 activation (Pelkey et al., 2006). In the same study, low concentrations of L-AP4 that would have preferentially activated mGluRs 4/8 had no effect on the calcium transients (Pelkey et al., 2006). Though our data indicate that the N-type VGCC can be a downstream target of mGluRs 4/8 activation, the complement of VGCCs linked to release is variable and application of low concentrations of L-AP4 may not result in a detectable change in calcium signal within the filopodial extensions.

Previous reports have indicated that group III mGluRs can inhibit transmitter release through targeting N-type VGCCs (Rusakov et al., 2004), P/Q-type VGCCs (Takahashi et al., 1996) and in a VGCC-independent mechanism (Scanziani et al., 1995; Schoppa and Westbrook, 1997; Woodhall et al., 2007). Application of ω-conotoxin GVIA to block N-type VGCCs partially occludes the actions of L-AP4 at the MF – L-Mi synapse. At ω-CgTx resistant synapses, where N-type VGCCs are not linked to glutamate release, however, L-AP4 is still effective. Our data also indicate that P/Q-type VGCCs are not likely to be a downstream target as ω-AgaTx did not occlude the actions of L-AP4. Consequently, it is likely that inhibition of glutamate release resulting from mGluRs 4/8 activation is mediated by at least two different mechanisms: one targeting release linked to N-type VGCCs, and a second VGCC-independent mechanism.

Since mGluRs 4/8 are negatively coupled to adenylyl cyclase (AC) and thus the associated intracellular cascade including cAMP and PKA (Anwyl, 1999; Cartmell and Schoepp, 2000), it is possible that proteins in the active zone release machinery, known to be sensitive to phosphorylation by PKA (e.g. RIM1α, CSP), are downstream targets of mGluRs 4/8 activation (Castillo et al., 2002; Evans et al., 2001; Leenders and Sheng, 2005). Interestingly, application of forskolin, an activator of AC, has been shown to induce a presynaptically-mediated potentiation at the MF to L-Mi connection (Galvan et al., 2010), demonstrating the potential importance of the AC / cAMP / PKA pathway in regulating synaptic transmission at the MF to L-Mi connection.

Additionally, though group II mGluRs are known to also be coupled to the AC pathway, it has been reported that group II mGLuRs do not modulate release from MF to interneurons through a cAMP pathway (Maccaferri et al., 1998). Together with our data showing a lack of occlusion of L-AP4 and DCG-IV at the MF – L-Mi connection and the further

demonstration of the independence of group II mGluRs from VGCCs as downstream targets, it seems that group II and group III mGluRs use different signaling cascades within MF boutons. This observation is in agreement with anatomical observations localizing the two receptor groups to different subcompartments of boutons, with group III mGluRs frequently localized to active zones, and group II mGluRs localized to periterminal regions (Corti et al., 2002; Shigemoto et al., 1997). Though understanding the full intracellular cascades for mGluR regulation of transmitter release from the MF is outside the scope of this study, it is certainly an interesting open question that deserves future attention.

Short term plasticity and mGluRs 4/8-mediated inhibition dictate MF output onto L-Mi

Previous reports have noted that interneurons do not tend to fire in response to a single input from MF granule cells, but that the probability of spike initiation increases throughout a train of high frequency stimuli (Henze et al., 2002; Lawrence et al., 2004). In keeping with these observations, L-Mi did not fire in response to a single MF stimulus but required a train of stimuli before reaching threshold. This is further supported by our data showing short term facilitation in response to short trains at 20 and 40 Hz. That MF input to L-Mi undergoes short term facilitation indicates that the individual synaptic inputs may be weak with a low P_r. This finding is consistent with our interpretation that individual MF inputs to L-Mi do not drive the interneuron because of the small quantal amplitude. Instead, convergence and summation of several MF inputs is required to elicit firing from the cell (Cosgrove et al., 2009).

Interestingly, high frequency presynaptic activities that are permissive for short term facilitation at the MF to L-Mi connection also are sufficient to activate presynaptic mGluRs 4/8 which, in turn, inhibit transmitter release. Since these receptors require a short burst of activity to become active and are not tonically active, the balance and timing between short term facilitation and inhibition of transmitter release from activation of mGluRs 4/8 is the result of complex presynaptic dynamics. For example, at 20 and 40 Hz, the inhibition by mGluRs 4/8 dictates the short term facilitation, reducing the amount of transmitter released during the train, thereby decreasing the amplitude and subsequent integration of the postsynaptic responses in the L-Mi. Indeed, when activation of mGluRs 4/8 was prevented by application of the competitive antagonist MSOP, enhanced short term facilitation was observed, the probability of spike transmission was higher, and the latency to first action potential was shorter. This delay in L-Mi firing caused by an mGluRs 4/8-mediated decrease in MF glutamate release means that additional synaptic input is required before summation of the inputs in the L-Mi is sufficient to elicit an action potential. Specifically, activation of mGluRs 4/8 delays L-Mi firing for tens to hundreds of milliseconds which, when a granule cell is firing at 20 or 40 Hz, corresponds to the requirement for several additional sequential synaptic events to fire the postsynaptic L-Mi (e.g. the leftward shift in the latency to first spike between MSOP and control conditions at 20Hz results in an interval difference of ~90 ms, which at 20 Hz would be equivalent to ~2 additional MF spikes). Thus, activation of mGluRs 4/8 imposes the requirement of longer and at higher frequency spike trains of MF input to elicit an action potential in the L-Mi. Thus, we hypothesize that activation of this receptor will have the largest impact during the physiological pattern of high frequency burst activity granule cells exhibit when a rat traverses a place field (Henze et al., 2002; Jung and McNaughton, 1993).

In contrast, at low frequencies of activity, mGluRs 4/8 do not become active and the strength of the connection is determined exclusively by the short term plasticity dynamics. MF synapses on pyramidal cells and str. lucidum interneurons undergo frequency facilitation (Henze et al., 2000; Salin et al., 1996; Scanziani et al., 1998; Toth et al., 2000) which is thought to allow for temporal integration of stimuli across a broad range of frequencies (Lawrence and McBain, 2003; Salin et al., 1996). Since baseline firing of granule cells is

usually low (Henze et al., 2002; Jung and McNaughton, 1993), frequency facilitation allows the MF connection to be sensitive to small changes in activity patterns (Lawrence and McBain, 2003; Salin et al., 1996). However, MF synapses on L-Mi do not facilitate at low or moderate frequencies, indicating that this connection may be responsive to the number rather than the frequency of active individual inputs.

Convergence of MF input to L-Mi

The range of quantal amplitudes recorded from L-Mi are significantly smaller than those reported in str. lucidum interneurons (Lawrence et al., 2004), and are closer to the range of amplitudes at the MF to pyramidal cell connection (Jonas et al., 1993) or the synaptic input to dentate gyrus granule cells (Bekkers and Clements, 1999). Previous reports on MF input to str. lucidum indicate that the individual synapses are strong but sparse (Lawrence et al., 2004; Lawrence and McBain, 2003). In contrast, based on an average EPSC amplitude that is approximately five times larger than the quantal amplitude, the MF input to L-Mi is relatively weak, but has a high convergence ratio (Table 1). Furthermore, MF EPSCs can be evoked in L-Mi from both the MF_{SDG} and MF_{SL} stimulation locations simultaneously (Cosgrove et al., 2009), indicating a greater degree of input convergence. It is interesting to note that failures were evident even with these EPSC amplitudes, possibly indicating a very low probability of release at each individual MF synapse. Together, these data indicate that MF input to L-Mi is comprised of many terminals with small quantal amplitudes and low probabilities of release.

Functional implications

Feedforward inhibition has been shown computationally to alter the relationship between synaptic input and action potential firing (Ferrante et al., 2009). In the absence of inhibition, the input/output (I/O) relationship of the pyramidal cell can be modeled by a single sigmoid function, with the lower limit set by the frequency of input required to reach action potential threshold, and the upper limit set by the maximum firing frequency of the cell. Because the activity of the interneuron can also be modeled by a sigmoid I/O function, when inhibition is added to the system the overall transfer function of the pyramidal cell is represented by the sum of both I/O curves (pyramidal cell and interneuron). The resultant biphasic sigmoid function has a plateau range at which the pyramidal cell could maintain a consistent output firing frequency across a wide range of input frequencies (Ferrante et al., 2009). By increasing the latency for eliciting spiking in the L-Mi, activation of mGluRs 4/8 shifts the I/O curve of the interneuron to the right. This rightward shift in the interneuron's I/O function effectively shifts the CA3 pyramidal cell I/O function to the right without changing the output frequency (Ferrante et al., 2009). This would allow a population of CA3 pyramidal cells receiving inhibitory input from interneurons with similar shifted I/O properties to fire at similar average frequencies regardless of input frequency ranges. Because the generation of oscillatory activity requires a rather homogeneous neuronal firing rate, activation of mGluRs 4/8 at MF terminals on feedforward interneurons could promote ensemble synchronization within the CA3 neural network.

Supplementary Material

Refer to Web version on PubMed Central for supplementary material.

Acknowledgments

Grant sponsor: NINDS, Grant number: NS24288 (GB), Grant sponsor: NSF, Grant number: 0844604 (SDM), Central Research Development Fund from the University of Pittsburgh.

References

Acsady L, Kamondi A, Sik A, Freund T, Buzsaki G. GABAergic cells are the major postsynaptic targets of mossy fibers in the rat hippocampus. J Neurosci. 1998; 18(9):3386–403. [PubMed: 9547246]

Alle H, Jonas P, Geiger JRP. PTP and LTP at a hippocampal mossy fiber-interneuron synapse. Proceedings of the National Academy of Sciences of the United States of America. 2001; 98(25): 14708–14713. [PubMed: 11734656]

Anwyl R. Metabotropic glutatmate receptors: electrophysiological properties and role in plasticity. Brain Research Reviews. 1999; 29(1):83–120. [PubMed: 9974152]

Ascoli GA, Brown KM, Calixto E, Card JP, Galván EJ, Perez-Rosello T, Barrionuevo G. Quantitative morphometry of electrophysiologically identified CA3b interneurons reveals robust local geometry and distinct cell classes. The Journal of Comparative Neurology. 2009; 515(6):677–695. [PubMed: 19496174]

Avoli M, D'Antuono M, Louvel J, Köhling R, Biagini G, Pumain R, D'Arcangelo G, Tancredi V. Network and pharmacological mechanisms leading to epileptiform synchronization in the limbic system in vitro. Progress in Neurobiology. 2002; 68(3):167–207. [PubMed: 12450487]

Bekkers JM, Clements JD. Quantal amplitude and quantal variance of strontium-induced asynchronous EPSCs in rat dentate granule neurons. The Journal of Physiology. 1999; 516(1):227–248. [PubMed: 10066937]

Billups B, Graham BP, Wong AYC, Forsythe ID. Unmasking group III metabotropic glutamate autoreceptor function at excitatory synapses in the rat CNS. The Journal of Physiology. 2005; 565(3):885–896. [PubMed: 15845577]

Bradley SR, Levey AI, Hersch SM, Conn PJ. Immunocytochemical localization of group III metabotropic glutamate receptors in the hippocampus with subtype-specific antibodies. J Neurosci. 1996; 16(6):2044–2056. [PubMed: 8604049]

Bradley SR, Standaert DG, Rhodes KJ, Rees HD, Testa CM, Levey AI, Conn PJ. Immunohistochemical localization of subtype 4a metabotropic glutamate receptors in the rat and mouse basal ganglia. The Journal of Comparative Neurology. 1999; 407(1):33–46. [PubMed: 10213186]

Breustedt J, Vogt KE, Miller RJ, Nicoll RA, Schmitz D. alpha1E-Containing Ca2+ channels are involved in synaptic plasticity. Proceedings of the National Academy of Sciences of the United States of America. 2003; 100(21):12450–12455. [PubMed: 14519849]

Calixto E, Galvan EJ, Card JP, Barrionuevo G. Coincidence detection of convergent perforant path and mossy fibre inputs by CA3 interneurons. J Physiol. 2008; 586(Pt 11):2695–712. [PubMed: 18388134]

Capogna M. Distinct properties of presynaptic group II and III metabotropic glutamate receptor-mediated inhibition of perforant pathway-CA1 EPSCs. European Journal of Neuroscience. 2004; 19(10):2847–2858. [PubMed: 15147318]

Cartmell J, Schoepp DD. Regulation of Neurotransmitter Release by Metabotropic Glutamate Receptors. Journal of Neurochemistry. 2000; 75(3):889–907. [PubMed: 10936169]

Castillo PE, Schoch S, Schmitz F, Sudhof TC, Malenka RC. RIM1[alpha] is required for presynaptic long-term potentiation. Nature. 2002; 415(6869):327–330. [PubMed: 11797010]

Castillo PE, Weisskopf MG, Nicoll RA. The role of Ca2+ channels in hippocampal mossy fiber synaptic transmission and long-term potentiation. Neuron. 1994; 12(2):261–269. [PubMed: 8110457]

Chen C-Y, Ling E-h, Horowitz JM, Bonham AC. Synaptic transmission in nucleus tractus solitarius is depressed by Group II and III but not Group I presynaptic metabotropic glutamate receptors in rats. The Journal of Physiology. 2002; 538(3):773–786. [PubMed: 11826164]

Conn PJ, Pin JP. Pharmacology and functions of metabotropic glutamate receptors. Annual Review of Pharmacology and Toxicology. 1997; 37(1):205–237.

Corti C, Aldegheri L, Somogyi P, Ferraguti F. Distribution and synaptic localisation of the metabotropic glutamate receptor 4 (mGluR4) in the rodent CNS. Neuroscience. 2002; 110(3):403–420. [PubMed: 11906782]

Cosgrove KE, Galván EJ, Meriney SD, Barrionuevo G. Area CA3 interneurons receive two spatially segregated mossy fiber inputs. Hippocampus. 2009; 9999:9999, NA.

de Jong AP, Verhage M. Presynaptic signal transduction pathways that modulate synaptic transmission. Current Opinion in Neurobiology. 2009; 19(3):245–253. [PubMed: 19559598]

Doherty J, Dingledine R. Differential Regulation of Synaptic Inputs to Dentate Hilar Border Interneurons by Metabotropic Glutamate Receptors. J Neurophysiol. 1998; 79(6):2903–2910. [PubMed: 9636096]

Evans GJO, Wilkinson MC, Graham ME, Turner KM, Chamberlain LH, Burgoyne RD, Morgan A. Phosphorylation of Cysteine String Protein by Protein Kinase A. Journal of Biological Chemistry. 2001; 276(51):47877–47885. [PubMed: 11604405]

Ferraguti F, Klausberger T, Cobden P, Baude A, Roberts JDB, Szucs P, Kinoshita A, Shigemoto R, Somogyi P, Dalezios Y. Metabotropic Glutamate Receptor 8-Expressing Nerve Terminals Target Subsets of GABAergic Neurons in the Hippocampus. J Neurosci. 2005; 25(45):10520–10536. [PubMed: 16280590]

Ferraguti F, Shigemoto R. Metabotropic glutamate receptors. Cell and Tissue Research. 2006; 326(2): 483–504. [PubMed: 16847639]

Ferrante M, Migliore M, Ascoli GA. Feed-forward inhibition as a buffer of the neuronal input-output relation. Proceedings of the National Academy of Sciences. 2009; 106(42):18004–18009.

Galvan EJ, Calixto E, Barrionuevo G. Bidirectional Hebbian Plasticity at Hippocampal Mossy Fiber Synapses on CA3 Interneurons. J Neurosci. 2008; 28(52):14042–14055. [PubMed: 19109487]

Galvan EJ, Cosgrove KE, Mauna JC, Card JP, Thiels E, Meriney SD, Barrionuevo G. Critical Involvement of Postsynaptic Protein Kinase Activation in Long-Term Potentiation at Hippocampal Mossy Fiber Synapses on CA3 Interneurons. J Neurosci. 2010; 30(8):2844–2855. [PubMed: 20181582]

Glitsch M. Selective Inhibition of Spontaneous But Not Ca2+-Dependent Release Machinery by Presynaptic Group II mGluRs in Rat Cerebellar Slices. J Neurophysiol. 2006; 96(1):86–96. [PubMed: 16611839]

Goda Y, Stevens C. Two components of transmitter release at a central synapse. Proceedings of the National Academy of Sciences of the United States of America. 1994; 91(26):12942–12946. [PubMed: 7809151]

Henze DA, Urban NN, Barrionuevo G. The multifarious hippocampal mossy fiber pathway: a review. Neuroscience. 2000; 98(3):407–427. [PubMed: 10869836]

Henze DA, Wittner L, Buzsaki G. Single granule cells reliably discharge targets in the hippocampal CA3 network in vivo. Nat Neurosci. 2002; 5(8):790–795. [PubMed: 12118256]

Jonas P, Major G, Sakmann B. Quantal components of unitary EPSCs at the mossy fibre synapse on CA3 pyramidal cells of rat hippocampus. J Physiol. 1993; 472:615–63. [PubMed: 7908327]

Jung MW, McNaughton BL. Spatial selectivity of unit activity in the hippocampal granular layer. Hippocampus. 1993; 3(2):165–182. [PubMed: 8353604]

Kamiya H, Shinozaki H, Yamamoto C. Activation of metabotropic glutamate receptor type 2/3 suppresses transmission at rat hippocampal mossy fibre synapses. J Physiol. 1996; 493 (Pt 2): 447–55. [PubMed: 8782108]

Knöpfel T, Uusisaari M. Modulation of Excitation by Metabotropic Glutamate Receptors. Inhibitory Regulation of Excitatory Neurotransmission. 2008:163–175.

Lacaille JC, Schwartzkroin PA. Stratum lacunosum-moleculare interneurons of hippocampal CA1 region. I. Intracellular response characteristics, synaptic responses, and morphology. J Neurosci. 1988; 8(4):1400–10. [PubMed: 3357023]

Lawrence JJ, Grinspan ZM, McBain CJ. Quantal transmission at mossy fibre targets in the CA3 region of the rat hippocampus. The Journal of Physiology. 2004; 554(1):175–193. [PubMed: 14678500]

Lawrence JJ, McBain CJ. Interneuron Diversity series: Containing the detonation -feedforward inhibition in the CA3 hippocampus. Trends in Neurosciences. 2003; 26(11):631–640. [PubMed: 14585604]

Leenders AGM, Sheng Z-H. Modulation of neurotransmitter release by the second messenger-activated protein kinases: Implications for presynaptic plasticity. Pharmacology & Therapeutics. 2005; 105(1):69–84. [PubMed: 15626456]

Li L, Bischofberger J, Jonas P. Differential Gating and Recruitment of P/Q-, N-, and R-Type Ca2+ Channels in Hippocampal Mossy Fiber Boutons. J Neurosci. 2007; 27(49):13420–13429. [PubMed: 18057200]

Lorez M, Humbel U, Pflimlin M-C, Kew JNC. Group III metabotropic glutamate receptors as autoreceptors in the cerebellar cortex. British Journal of Pharmacology. 2003; 138(4):614–625. [PubMed: 12598415]

Losonczy A, Somogyi P, Nusser Z. Reduction of Excitatory Postsynaptic Responses by Persistently Active Metabotropic Glutamate Receptors in the Hippocampus. J Neurophysiol. 2003; 89(4): 1910–1919. [PubMed: 12686572]

Maccaferri G, Toth K, McBain CJ. Target-specific expression of presynaptic mossy fiber plasticity. Science. 1998; 279(5355):1368–70. [PubMed: 9478900]

Macek TA, Winder DG, Gereau RW, Ladd CO, Conn PJ. Differential involvement of group II and group III mGluRs as autoreceptors at lateral and medial perforant path synapses. J Neurophysiol. 1996; 76(6):3798–3806. [PubMed: 8985877]

Manzoni OJ, Castillo PE, Nicoll RA. Pharmacology of metabotropic glutamate receptors at the mossy fiber synapses of the guinea pig hippocampus. Neuropharmacology. 1995; 34(8):965–971. [PubMed: 8532177]

Miyazaki K, Ishizuka T, Yawo H. Synapse-to-synapse variation of calcium channel subtype contributions in large mossy fiber terminals of mouse hippocampus. Neuroscience. 2005; 136(4): 1003–1014. [PubMed: 16226383]

Ohishi H, Akazawa C, Shigemoto R, Nakanishi S, Mizuno N. Distribution of the mRNAs for L-2-amino-4-phosphonobutyrate-sensitive metabotropic glutatmate receptors, mGluR4 and mGluR7, in the rat brain. Journal of Comparative Neurology. 1995; 360(4):555–570. [PubMed: 8801249]

Pelkey KA, Lavezzari G, Racca C, Roche KW, McBain CJ. mGluR7 is a metaplastic switch controlling bidirectional plasticity of feedforward inhibition. Neuron. 2005; 46(1):89–102. [PubMed: 15820696]

Pelkey KA, Topolnik L, Lacaille JC, McBain CJ. Compartmentalized Ca2+ Channel Regulation at Divergent Mossy-Fiber Release Sites Underlies Target Cell-Dependent Plasticity. Neuron. 2006; 52(3):497–510. [PubMed: 17088215]

Perkins KL. Cell-attached voltage-clamp and current-clamp recording and stimulation techniques in brain slices. Journal of Neuroscience Methods. 2006; 154(1–2):1–18. [PubMed: 16554092]

Price CJ, Karayannis T, Pál BZ, Capogna M. Group II and III mGluRs-mediated presynaptic inhibition of EPSCs recorded from hippocampal interneurons of CA1 stratum lacunosum moleculare. Neuropharmacology. 2005; 49(Supplement 1):45–56. [PubMed: 15998525]

Rusakov DA, Wuerz A, Kullmann DM. Heterogeneity and Specificity of Presynaptic Ca2+ Current Modulation by mGluRs at Individual Hippocampal Synapses. Cereb Cortex. 2004; 14(7):748–758. [PubMed: 15054054]

Salin PA, Scanziani M, Malenka RC, Nicoll RA. Distinct short-term plasticity at two excitatory synapses in the hippocampus. Proceedings of the National Academy of Sciences of the United States of America. 1996; 93(23):13304–13309. [PubMed: 8917586]

Saugstad JA, Kinzie JM, Mulvihill ER, Segerson TP, Westbrook GL. Cloning and expression of a new member of the L-2-amino-4-phosphonobutyric acid-sensitive class of metabotropic glutamate receptors. Molecular Pharmacology. 1994; 45(3):367–372. [PubMed: 8145723]

Saugstad JA, Kinzie JM, Shinohara MM, Segerson TP, Westbrook GL. Cloning and Expression of Rat Metabotropic Glutamate Receptor 8 Reveals a Distinct Pharmacological Profile. Molecular Pharmacology. 1997; 51(1):119–125. [PubMed: 9016353]

Scanziani M, Gahwiler BH, Charpak S. Target cell-specific modulation of transmitter release at terminals from a single axon. Proceedings of the National Academy of Sciences of the United States of America. 1998; 95(20):12004–12009. [PubMed: 9751780]

Scanziani M, Gahwiler BH, Thompson SM. Presynaptic inhibition of excitatory synaptic transmission by muscarinic and metabotropic glutamate receptor activation in the hippocampus: are Ca2+ channels involved? Neuropharmacology. 1995; 34(11):1549–1557. [PubMed: 8606802]

Scanziani M, Salin PA, Vogt KE, Malenka RC, Nicoll RA. Use-dependent increases in glutamate concentration activate presynaptic metabotropic glutamate receptors. Nature. 1997; 385(6617): 630–634. [PubMed: 9024660]

Schoepp DD. Unveiling the Functions of Presynaptic Metabotropic Glutamate Receptors in the Central Nervous System. Journal of Pharmacology and Experimental Therapeutics. 2001; 299(1):12–20. [PubMed: 11561058]

Schoppa NE, Westbrook GL. Modulation of mEPSCs in Olfactory Bulb Mitral Cells by Metabotropic Glutamate Receptors. J Neurophysiol. 1997; 78(3):1468–1475. [PubMed: 9310436]

Semyanov A, Kullmann DM. Modulation of GABAergic signaling among interneurons by metabotropic glutamate receptors. Neuron. 2000; 25(3):663–72. [PubMed: 10774733]

Shigemoto R, Kinoshita A, Wada E, Nomura S, Ohishi H, Takada M, Flor PJ, Neki A, Abe T, Nakanishi S, et al. Differential presynaptic localization of metabotropic glutamate receptor subtypes in the rat hippocampus. J Neurosci. 1997; 17(19):7503–22. [PubMed: 9295396]

Takahashi T, Forsythe I, Tsujimoto T, Barnes-Davies M, Onodera K. Presynaptic calcium current modulation by a metabotropic glutamate receptor. Science. 1996; 274(5287):594–597. [PubMed: 8849448]

Tanabe Y, Nomura A, Masu M, Shigemoto R, Mizuno N, Nakanishi S. Signal transduction, pharmacological properties, and expression patterns of two rat metabotropic glutamate receptors, mGluR3 and mGluR4. J Neurosci. 1993; 13(4):1372–1378. [PubMed: 8463825]

Tang F. Agonists and antagonists of metabotropic glutamate receptors: anticonvulsants and antiepileptogenic agents? Current Neuropharmacology. 2005; 3(4):299–307. [PubMed: 18369399]

Thomas NK, Jane DE, Tse HW, Watkins JC. [alpha]-methyl derivatives of serine-O-phosphate as novel, selective competitive metabotropic glutamate receptor antagonists. Neuropharmacology. 1996; 35(6):637–642. [PubMed: 8887973]

Toth K, McBain CJ. Afferent-specific innervation of two distinct AMPA receptor subtypes on single hippocampal interneurons. Nat Neurosci. 1998; 1(7):572–8. [PubMed: 10196564]

Toth K, McBain CJ. Target-specific expression of pre- and postsynaptic mechanisms. The Journal of Physiology. 2000; 525(1):41–51. [PubMed: 10811723]

Toth K, Suares G, Lawrence JJ, Philips-Tansey E, McBain CJ. Differential mechanisms of transmission at three types of mossy fiber synapse. J Neurosci. 2000; 20(22):8279–89. [PubMed: 11069934]

von Gersdorff H, Schneggenburger R, Weis S, Neher E. Presynaptic Depression at a Calyx Synapse: The Small Contribution of Metabotropic Glutamate Receptors. J Neurosci. 1997; 17(21):8137–8146. [PubMed: 9334389]

Williams S, Samulack DD, Beaulieu C, LaCaille JC. Membrane properties and synaptic responses of interneurons located near the stratum lacunosum-moleculare/radiatum border of area CA1 in whole-cell recordings from rat hippocampal slices. J Neurophysiol. 1994; 71(6):2217–35. [PubMed: 7931512]

Woodhall GL, Ayman G, Jones RSG. Differential control of two forms of glutamate release by group III metabotropic glutamate receptors at rat entorhinal synapses. Neuroscience. 2007; 148(1):7–21. [PubMed: 17630217]

Yoshino M, Sawada S, Yamamoto C, Kamiya H. A metabotropic glutamate receptor agonist DCG-IV suppresses synaptic transmission at mossy fiber pathway of the guinea pig hippocampus. Neuroscience Letters. 1996; 207(1):70–72. [PubMed: 8710213]

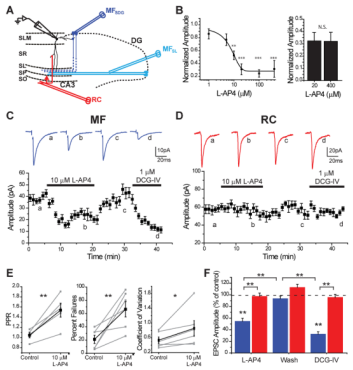

Figure 1. High affinity group III mGluRs are present of MF terminals contacting L-Mi

A) Schematic drawing showing the placement of recording and stimulating electrodes. Recordings were made from interneurons with soma in the str. lacunosum moleculare of area CA3. Extracellular stimulating electrodes were placed either at the medial extent of the suprapyramidal blade of the dentate gyrus (MF_{SDG}), within the str. lucidum (MF_{SL}), or in the str. oriens of CA3 (RC). Abbreviations: SO: str. oriens; SP: str. pyramidale; SL: str. lucidum; SR: str. radiatum; SLM: str. lacunosum moleculare; DG: dentate gyrus. B) Plot of normalized EPSC amplitude at varying concentrations of L-AP4 from 1 to 400 μM. Summary bar graph demonstrating no difference in the amount of inhibition by 20 vs. 400 μM L-AP4. N ≥ 5 at each point. C) Example cell showing the effect of 10 μM L-AP4 on MF evoked EPSCs. Each symbol is the average of 5 consecutive EPSCs. Averaged traces (N = 30) are inset; a = control, b = L-AP4, c = washout, d = DCG-IV. D) Same as in C, but as a result of RC stimulation. E) Summary data for paired-pulse ratio (left), failure rate (middle) and coefficient of variation (right) of a subset of the data. F) Summary data showing the effect of 10 μM L-AP4 on MF evoked (blue bars, N = 11) and RC evoked (red bars, N = 6) EPSCs. *p < 0.05; **p < 0.01; ***p < 0.001

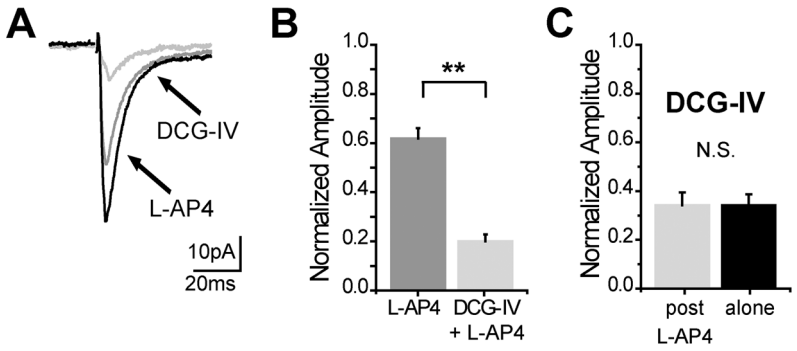

Figure 2. L-AP4 does not occlude DCG-IV

A) Averaged traces (N = 30) of a MF EPSC after application of 10 μM L-AP4 (dark grey) and then 1 μM DCG-IV (light grey) in the continued presence of L-AP4. B) Summary data showing the average normalized values following L-AP4 (dark grey bar) and DCG-IV (light grey bar) in the continued presence of L-AP4. C) Summary data comparing the effect of DCG-IV after L-AP4 (light grey bar) vs. DCG-IV alone (black bar, data re-presented from Fig. 11) on the normalized value of EPSC amplitude. There was no difference in the effect of DCG-IV ($p > 0.001$). **$p < 0.01$

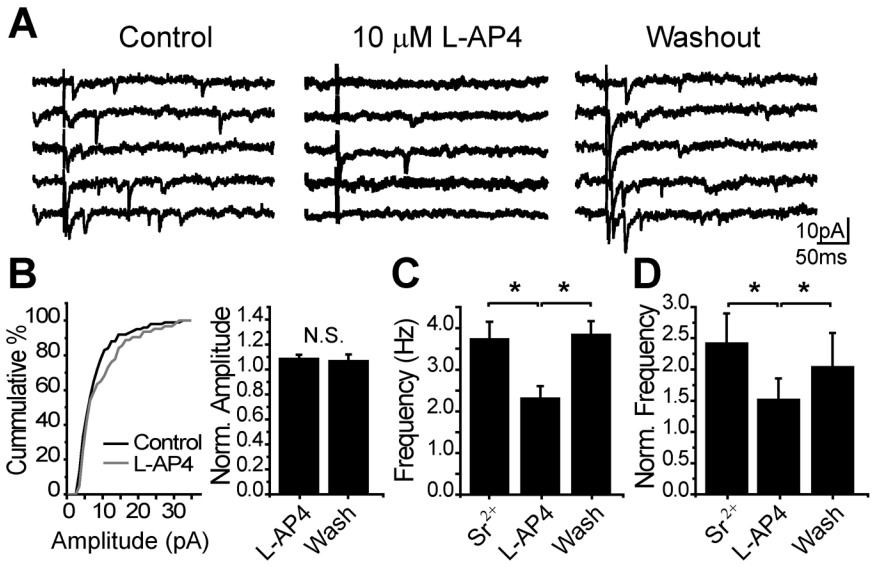

Figure 3. L-AP4 decreases frequency but not amplitude of aEPSCs

A) Sample traces recorded from a representative L-Mi in the presence of 3 mM Sr^{2+} (left), 10 μM L-AP4 (middle), and following L-AP4 wash out (right). B) Left, plot of the cumulative amplitude of aEPSCs before (control, black line) and after L-AP4 (grey line) for the example cell. No significant difference was observed in the amplitude distribution ($p = 0.198$; K-S test). Right, summary data of the average amplitude of aEPSCs normalized to the amplitude of aEPSCs in the control condition. There is no significant difference in amplitude with L-AP4, or washout. C and D) L-AP4 decreases both the actual frequency of aEPSCs (C) and the frequency of aEPSCs when normalized to the spontaneous frequency (D). *$p < 0.05$

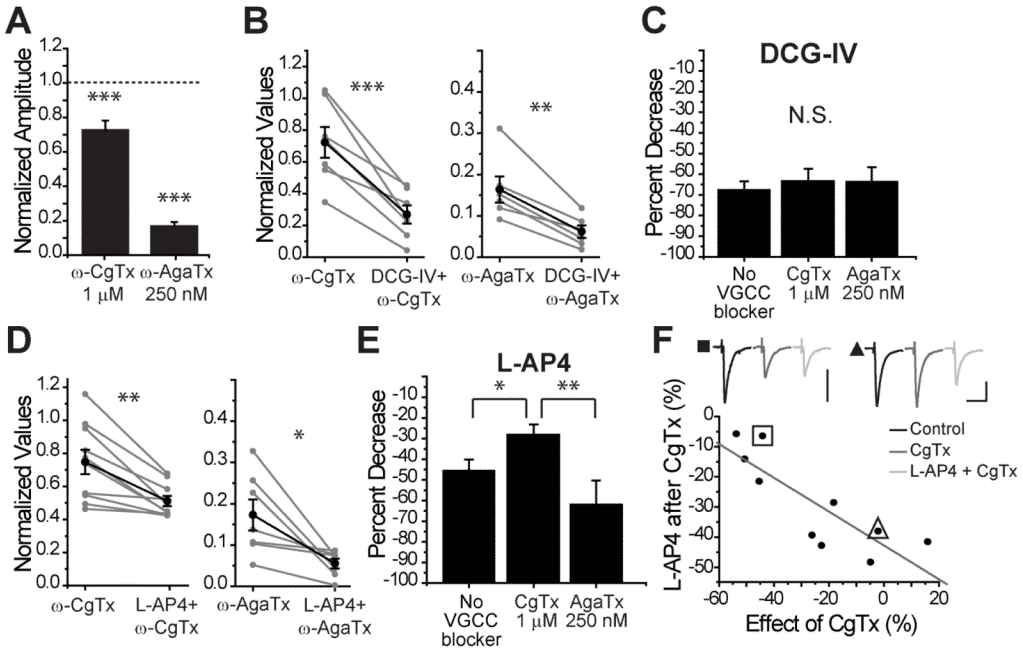

Figure 4. Group III mGluR activation targets glutamate release linked to N-type VGCCs

A) Summary bar graph of normalized EPSC amplitudes following application of VGCC blockers. Glutamate release from the MF is linked to P/Q-type (AgaTx sensitive) and N-type (CgTx sensitive) VGCCs. B and D) Normalized amplitudes following application of specific VGCC blockers CgTx (left) and AgaTx (right) and subsequent application of DCG-IV (B) or L-AP4 (D). Grey lines and symbols represent individual cell data, with black lines and symbols representing averaged data. C and E) Summary bar graphs showing the effect of DCG-IV (C) or L-AP4 (E) alone (re-plotted from Figure 1, left bar), and in the continued presence of CgTx (middle bar) or AgaTx (right bar). No difference in the percent decrease as a result of DCG-IV application was observed. In contrast, the effect of L-AP4 following application of CgTx is partially occluded, as the percent decrease following L-AP4 in the continued presence of CgTx is less than the effect of L-AP4 alone and the effect of L-AP4 in the continued presence of AgaTx. F) Scatter plot of the effect of L-AP4 in the continued presence of CgTx vs. the effect of CgTx alone. Symbols represent individual cells, which are fit with a regression line (grey line), showing a significant correlation ($R = -0.807$; $p < 0.01$). Inset are two sets of averaged traces (N= 30) from representative cells having a large CgTx effect (square, left) and a small CgTx effect (triangle, right). Control EPSCs are represented in black (left), with CgTx treatment in dark grey (middle) and L-AP4 in the continued presence of CgTx in light grey (right). When the CgTx effect was large, L-AP4 did not have any additional effect, as represented by the cell denoted by the square. Scale bars: 20 pA, 25 ms. *** $p < 0.001$; ** $p < 0.01$; * $p < 0.05$.

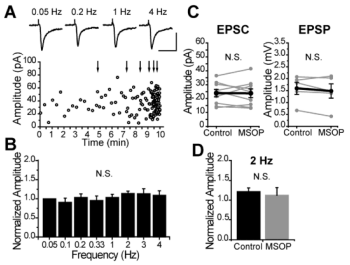

Figure 5. Group III mGluRs are neither tonically active nor activated by low frequency activity

A) Averaged traces (N = 15) from a representative cell (top) and a scatter plot of EPSC amplitudes over time across all test frequencies (bottom). Arrows indicate a change in stimulation frequency from 0.05 to 0.1, 0.2, 0.33, 1, 2 and 4 Hz. B) Plot of MF evoked EPSCs at 0.1, 0.2, 0.33, 1, 2, 3, and 4 Hz normalized to EPSCs evoked at 0.05 Hz. No significant increase in EPSC amplitude was seen at any frequency ($N \geq 7$ for all frequencies; $p > 0.5$). C) Effect of MSOP on the amplitude of single EPSCs (left) and EPSPs (right). Individual cell data is represented by grey symbols and lines, averaged data (mean ± SEM) is represented by black symbols and lines. D) Application of MSOP does not reveal frequency facilitation at 2 Hz. Plot of EPSC amplitude normalized to 0.05 Hz control under both control and MSOP conditions. There were no significant differences between control and MSOP at 2Hz ($N = 5$; $p = 0.677$) and neither the control nor the MSOP condition was significantly different than the 0.05 Hz control ($N = 5$; $p > 0.05$).

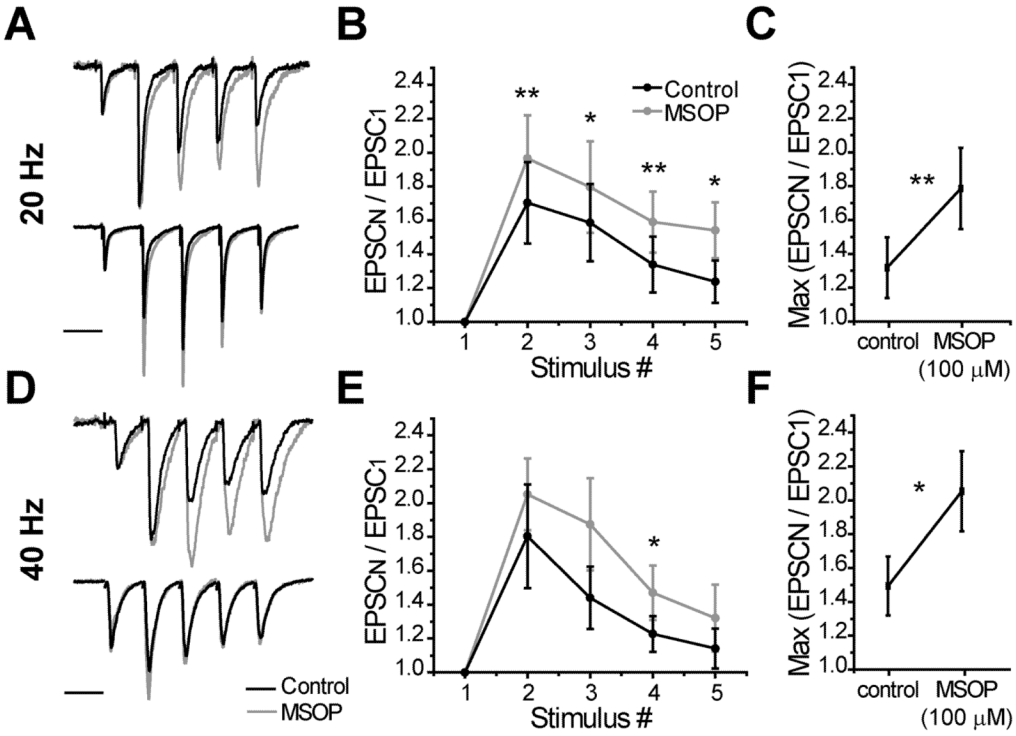

Figure 6. Relief of inhibition mediated by mGluRs 4/8 using the selective receptor antagonist MSOP reveals enhanced facilitation during short, high frequency trains

EPSCs were evoked by short trains of MF stimulation at 20 Hz (A) and 40 Hz (D). Sample traces in A and D are average EPSCs (N = 10 – 15) from two representative cells before (black trace) and after (grey trace) MSOP application illustrating the variability in facilitation pattern and timing of the effect of MSOP. The first EPSCs were normalized to allow comparison between conditions. B and E) Summary plot of the ratio of $EPSC_N$ / $EPSC_1$ for each stimulus before (black line and symbols) and after application of 100 μM MSOP (grey line and symbols). Traces were normalized to the first EPSC of the control condition for each cell in the average. C and F) Plot of the ratio of $EPSC_N$ / $EPSC_1$ at the stimulus number that had the largest effect of MSOP (e.g. in A, top set of traces, $EPSC_5$ / $EPSC_1$, bottom set of traces, $EPSC_2$ / $EPSC_1$) **p < 0.01; *p < 0.05.

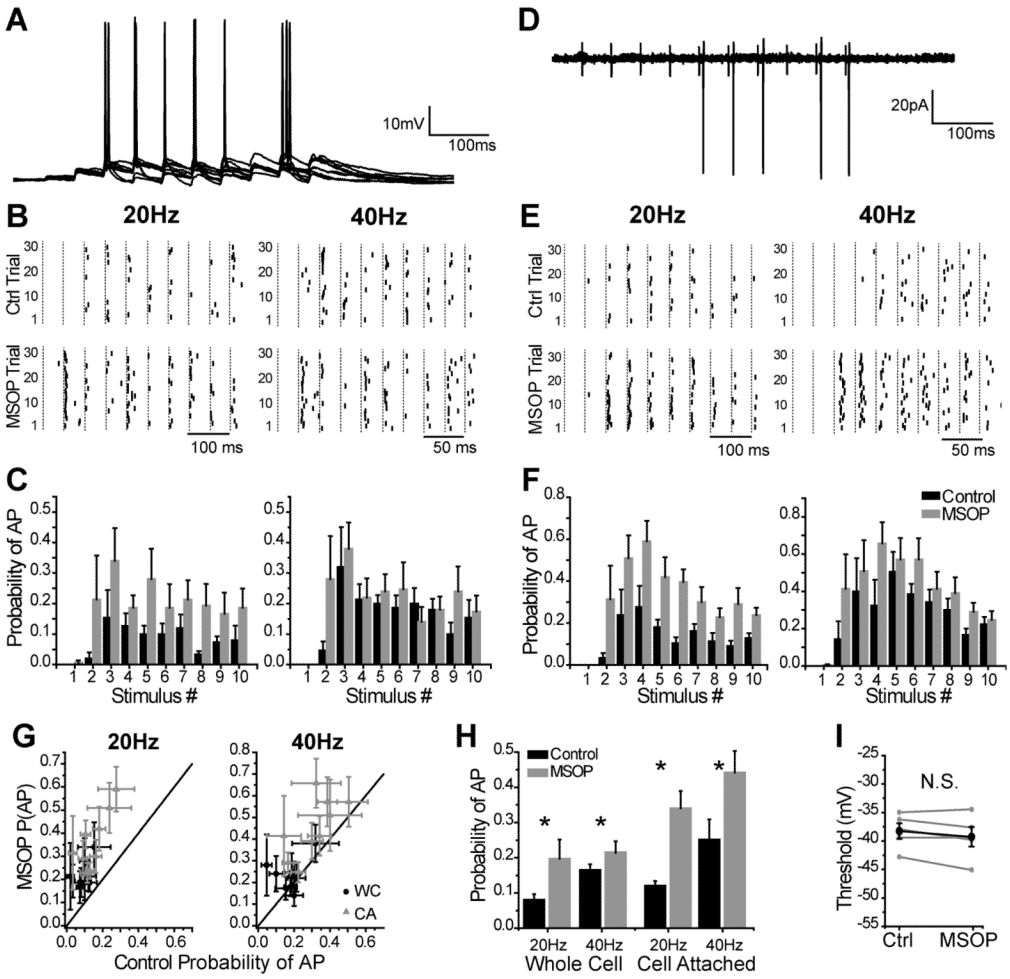

Figure 7. Activation of presynaptic group III mGluRs decreases the probability of AP firing in L-Mi in response to trains of MF input

A to C) MSOP application increases the probability of L-Mi firing in response to trains of MF input at 20 and 40 Hz. A) Example traces recorded from an L-Mi in response to trains of ten stimuli. B) Raster plots showing occurrence of AP firing in response to 30 trains of 10 stimuli at 20 (left) and 40 Hz (right) before (top row) and after MSOP application (bottom row). Each tick mark represents a single action potential. Vertical dotted lines indicate the time of each stimulus. C) Plots of the probability of AP firing in response to a train of ten stimuli at 20 and 40 Hz when recorded in whole cell patch clamp configuration. Black bars are control probabilities, grey bars are probabilities after application of MSOP. D to F) Same as A through C but in cell attached patch clamp recording configuration. G) Plot of the probability of action potential firing in the presence of MSOP vs. the probability of an AP in control conditions at 20 (left) and 40 Hz (right). Black line is the unity line. (•) represents whole cell. (Δ) represents the cell attached. H) Summary plot of the overall probability of action potential firing at 20 and 40 Hz. Black bars are control, grey bars are MSOP. MSOP application increases the probability of AP firing in all conditions. I) Plot of AP threshold before and after application of MSOP. There was no significant difference after application of MSOP. *$p < 0.05$

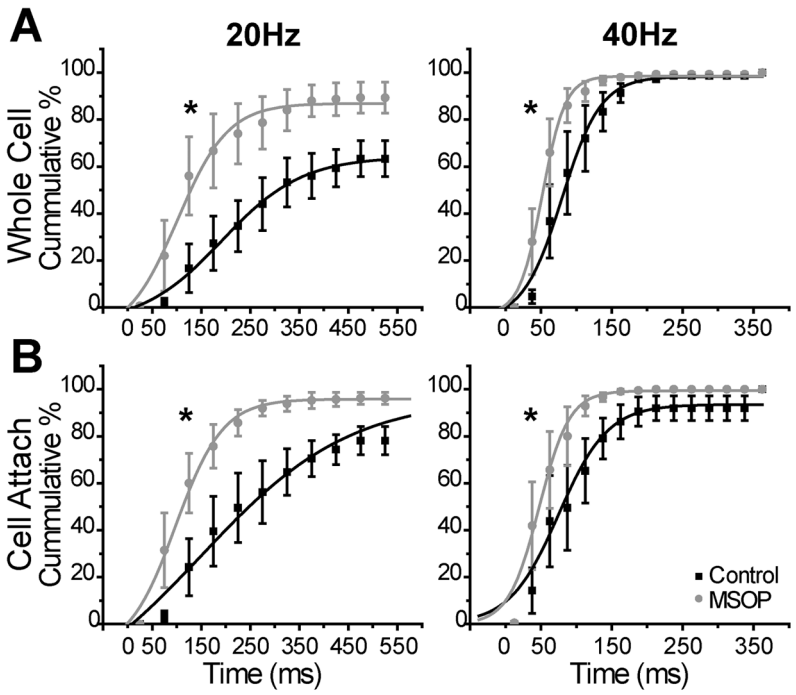

Figure 8. Activation of group III mGluRs delays L-Mi firing in response to a train of MF stimulation

A) Summary data plotting the cumulative probability of the latency to the first AP in each train at 20 and 40 Hz for whole cell and cell attach (B) condition before (black dots and fits) and after (grey dots and fits) MSOP application at both 20 (left) and 40 Hz (right). Scatter plots were then fit with a Boltzmann function. *$p < 0.05$

Table 1

MF_{SDG} and MF_{SL} input to L-Mi are not different

No differences in the characteristics of EPSCs evoked from the MF_{SDG} vs. MF_{SL} stimulation locations were detected, including sensitivity to the group II agonist DCG-IV, and the group III agonist L-AP4.

	MF_{SDG} (N = 52)	MF_{SL} (N = 29)	p value
Amplitude (pA)	35.07 ± 6.15	37.53 ± 2.94	0.772
Quantal Amplitude (pA)	7.72 ± 0.44 (N = 6)	8.12 ± 0.36 (N = 4)	0.541
Rise time (ms)	1.27 ± 0.06	1.34 ± 0.14	0.604
Decay tau (ms)	6.99 ± 0.40	7.70 ± 0.96	0.430
PPR	1.75 ± 0.11	1.78 ± 0.16	0.883
Sensitivity to 10 μM L-AP4 (% of control)	58.43 ± 3.34% (N =17)	53.65 ± 6.08% (N = 11)	0.461
Sensitivity to 1–2.5 μM DCG-IV (% of control)	30.15 ± 2.48% (N = 22)	37.51 ± 4.29% (N = 12)	0.140